



Open Archive TOULOUSE Archive Ouverte (OATAO)

OATAO is an open access repository that collects the work of Toulouse researchers and makes it freely available over the web where possible.


This is an author-deposited version published in : <http://oatao.univ-toulouse.fr/>
Eprints ID : 17606

To link to this article : DOI : 10.1111/jace.14451
URL : <http://dx.doi.org/10.1111/jace.14451>

<p>To cite this version : Duluard, Sandrine and Paillassa, Aude and Lenormand, Pascal and Taberna, Pierre-Louis and Simon, Patrice and Rozier, Patrick and Ansart, Florence <i>Dense on Porous Solid LATP Electrolyte System: Preparation and Conductivity Measurement</i>. (2016) Journal of American Ceramic Society, vol.100, n°1, pp. 141-149. ISSN 0002-7820</p>
--

Any correspondence concerning this service should be sent to the repository administrator: staff-oatao@listes-diff.inp-toulouse.fr

Dense on porous solid LATP electrolyte system: Preparation and conductivity measurement

Sandrine Duluard  | Aude Paillassa | Pascal Lenormand | Pierre-Louis Taberna |
Patrice Simon | Patrick Rozier | Florence Ansart

CIRIMAT, Université de Toulouse, CNRS, INPT, UPS, Université Toulouse 3 Paul Sabatier, F-31062 Toulouse Cedex 9 - Réseau sur le Stockage Electrochimique de l'Energie (RS2E), FR CNRS 3459, Toulouse, France

Correspondence

Sandrine Duluard, CIRIMAT, Université de Toulouse, CNRS, INPT, UPS, Université Toulouse 3 Paul Sabatier, F-31062 Toulouse Cedex 9 - Réseau sur le Stockage Electrochimique de l'Energie (RS2E), FR CNRS 3459, Toulouse, France.
Email: duluard@chimie.ups-tlse.fr

Abstract

A dense membrane of lithium aluminum titanium phosphate $\text{Li}_{1+x}\text{Al}_x\text{Ti}_{2-x}(\text{PO}_4)_3$, $x=0.3$ (LATP) is deposited on a porous LATP substrate via wet chemistry. In the polymerized complex process, phosphate precursors with different active groups and steric hindrance are selected to tune precursor's reactivity. Rheological studies and microstructural observations lead to the selection of an LATP powder slurry charged with lithium, aluminum, titanium, and phosphate ion precursors. The optimized formulation is impregnated into a porous LATP substrate. After thermal treatment, dense LATP membranes on top of a porous LATP substrate are obtained with conductivities as high as 3×10^{-4} S/cm for the dense part, the porous part acting as a mechanical support. An original Van der Pauw impedance setup is validated for the measurement of the ionic conductivity of such dense/porous systems.

KEYWORDS

densification, dual system, sol-gel transition, solid electrolyte, Van der Pauw impedance

1 | INTRODUCTION

With a theoretical energy density of 500-900 Wh/kg,¹ lithium-air batteries are being investigated for next generations of electrical vehicles. Among the two main technologies differing by the nature of the electrolyte (aqueous vs organic), aqueous lithium-air systems allowing the use of nontreated air offers the advantage of using oxygen electrode technology already developed for fuel cells applications. To reach high capacities, one of the main challenges is the development of a solid electrolyte membrane acting as an efficient physical barrier to water, to prevent the oxidation of lithium while providing a high lithium transfer number.

Among highly conductive lithium electrolytes, air stable electrolytes are selected for practical considerations including the simplification of batteries production process and cost lowering. Lithium aluminum titanium phosphates (LATP) are one of the best candidates due to their

conductivity as high as 3×10^{-4} S/cm² for the optimized composition $\text{Li}_{1+x}\text{Al}_x\text{Ti}_{2-x}(\text{PO}_4)_3$ $x=0.3$. A large number of preparation methods are reported for LATP powders in the literature, from solid-state reactions³⁻⁵ that could be followed by a mechanical activation,⁶ to sol-gel⁷⁻⁹ possibly associated with a 3D shaping,¹⁰ co-precipitation,¹¹⁻¹³ or hydrothermal reaction.¹⁴ In all cases, extra treatments are then applied for shaping and sintering. It is worth noting that in the literature the preparation method slightly impacts the conductivity values, with values ranging from a 0.4 to 7×10^{-4} S/cm total conductivity for solid-state syntheses and from 0.1 to 7×10^{-4} from wet chemistry routes.

Membranes as thin as possible should be prepared to lower the area-specific resistance. Two main preparation methods are reported in the literature: the preparation of slices from a bulk material and the preparation of greens from powder dispersion and subsequent sintering. In a previous work, we prepared dense and highly conductive self-supporting LATP membranes via Spark Plasma Sintering,

with the required thickness after polishing.¹⁵ A solid-state protocol has been also developed by OHARA¹⁶ for the preparation of solid electrolytes. However, these processes are time and material consuming, not suitable for very thin membranes and not convenient for in line production. In some cases low thickness greens can be obtained, but their mechanical properties after sintering are not optimized. One main challenge is to prepare an electrolyte dense enough to get high conductivity and water tightness, and thin enough to have low ionic resistance.

To overcome this challenge and reach a compromise between high mechanical performance and low ionic resistance, we propose a dual system electrolyte made with a thin membrane which insures the physical barrier function deposited on a porous substrate acting as a mechanical support. The membrane deposition method is not impacted by the thickness of the porous support so that this support can be chosen as thick as necessary to get the required mechanical strength. Such configuration is developed for SOFC application, the porous current collector acting also as mechanical support for the whole SOFC stack (3rd gen.).¹⁷

In this work, the membrane was prepared via deposition of a thin layer of LATP on an optimized LATP porous substrate followed by thermal treatment to ensure the densification of the film. The sintering treatment should be limited in temperature (below 1100°C) and duration to limit lithium sublimation and subsequent decrease in the ionic conductivity. To densify the coating at rather low temperature, LATP precursors in the form of a polymerized complex sol were added in stoichiometric proportions to the LATP dispersion expecting the formation of ceramic bridges between LATP grains known to improve densification process as already demonstrated by our laboratory with other types of materials including yttria-stabilized zirconia.¹⁸

To reach this objective, different challenges have to be overcome. First, a homogeneous distribution of the precursors in the LATP precursor's solution should be obtained to ensure stoichiometric formation of LATP at the bridges. In the literature, alkoxides route tested by Cretin et al.¹⁹ resulted in LATP precipitation instead of sol-gel transition and variations in the experimental conditions by Wu et al.²⁰ did not result in a homogeneous sol. Here, we chose to develop a protocol based on the polymerized complex method, ie, formation of a complex between metallic salts and a gel forming chelating agent. This method is dedicated to the preparation of a sol with homogeneously dispersed salts and has been used for the preparation of a large variety of materials including single oxides and mixed oxides such as YSZ,²¹ $\text{La}_{0.4}\text{Sr}_{0.6}\text{Co}_{0.8}\text{Fe}_{0.2}\text{O}_{3-\delta}$,²² $\text{La}_2\text{NiO}_{4+\delta}$,²³ and PMN-PT.²⁴ The second challenge is the preparation of a crystallized LATP powder without the formation of secondary phases

at the grain boundary often reported to be detrimental to the overall conductivity.⁶ The third challenge is to prepare samples with mastered grain size in the range of hundreds of nm which is a compromise between grain size large enough to favor high conductivity, as LATP conductivity is mainly driven by the grain bulk conductivity, and sub-micronic grain size (<1.6 μm) to avoid microcracking in the film.²⁵

The effectiveness of both physical barrier effect and high ionic conductivity of the membrane was investigated by conventional method for the former and for the later via the adaptation with impedance setup of the Van der Pauw method to take into account the dual dense/porous character of the system.

The scope of this study is then to describe that an optimized thermal treatment of the deposition of a dispersion of LATP powder and polymerized precursors onto a porous substrate allows the formation of dense and highly conductive LATP membranes.

2 | EXPERIMENTAL PROCEDURE

2.1 | Raw materials

Aluminum nitrate nonahydrated (>98%, Fisher Scientific, Illkirch, France), titanium (III) chloride solution at 20% in water (Sigma Aldrich, Saint-Quentin Fallavier, France), lithium acetate dihydrate ($\geq 99\%$, Sigma Aldrich), hexamethylenetetramine (99%, Acros Organics, Geel, Belgium), acetylacetone (>99%, Sigma-Aldrich), acetic acid (100%, VWR), phosphoric acid (VWR), trimethylphosphate ($\geq 97\%$, Aldrich), triethylphosphate ($\geq 99.8\%$, Aldrich), 2-butanone (99%, Acros Organics), absolute ethanol (VWR), and polyvinylpyrrolidone PVP K12 dispersant (Acros Organics, Average Mw=3500) were used as raw precursors.

Porous LATP substrates were prepared by CTI (Ceramiques Techniques Industrielles, Salindres, France) from LATP powder (protocol for the powder preparation described elsewhere¹⁵) by addition of 5% starch porous agent to the powder before pressing and sintering at 1000°C during 1 hour. Pellets with diameter 12 mm and 30%-40% v/v porosity with 1-2 μm pore size were obtained by CTI.

2.2 | Characterizations

Phase identification was carried out by X-Ray Diffraction (Bruker D4 Endeavor, Bruker AXS, Mame-la-Vallée, France) using a CuK_α radiation source ($K_\alpha=0.154$ 18 nm). Scanning electron microscope with Field Emission Gun (JEOL JSM 6700F, JEOL Europe SAS, Croissy, France) with a 5 kV accelerating voltage was used for morphological and microstructural investigations. The rheological properties of the precursor solutions were measured by a

viscosimeter (Lamy Rheology model TVe-05, Champagne-au-Mont-d'Or, France) with shear rate from 320 to 4500 seconds⁻¹. For the dispersions (low quantities available, 2-3 mL), another viscosimeter (Anton Paar Physica MCR301, Les Ulis, France) was used in a cone and plate configuration equipped with a solvent trap. Impedance measurements were performed with frequencies ranging from 10⁷ to 1 Hz (Solartron 1260 AMETEK France, Elancourt, France).

2.3 | Preparation of the dual dense/porous system

2.3.1 | Schematic of the preparation procedure

The preparation procedure for the dual system is summarized in the diagram Figure 1. Details for each step are given in the following paragraphs.

2.3.2 | Polymerized complex sols preparation (sol 1A, 1B, 1C)

Lithium aluminum titanium phosphates sols were synthesized via a polymerized complex method. An aqueous

solution at 0.64 mol·L⁻¹ total molar concentration in metallic ions was prepared with convenient stoichiometry of lithium, aluminum, titanium from lithium acetate dehydrate, aluminum nitrate nonahydrated, and titanium (III) chloride solution. On the other hand, a solution of 0.85 mol·L⁻¹ total molar concentration in hexamethylenetetramine (HMTA) and acetylacetonate (Acac) in acetic acid was prepared with a molar ratio HMTA/Acac equal to 1. The solution was stirred for 2 hour until an orange color, characteristic of the opening of the HMTA cycles, appears. The two solutions were mixed in proportions such that the molar ratio ([HMTA] + [Acac])/[Metallic ions] be equal to 4. The phosphate precursor was then added under stirring. After thermal treatment at 80°C during 45 minute, a polymeric matrix was obtained from polymerization and polycondensation reactions between HMTA and Acac. Liquid phosphate precursors with different reactivity and steric hindrance were chosen: phosphoric acid (H₃PO₄) and trimethylphosphate [(CH₃)₃PO₄] and triethylphosphate [(C₂H₅)₃PO₄] phosphate esters. Thus, we obtained three types of sol of LATP precursors dispersed into a polymeric matrix with different phosphate precursors. For sake of clarity, the sols with H₃PO₄, (CH₃)₃PO₄, and (C₂H₅)₃PO₄ precursors are named sol 1A, sol 1B, and sol 1C, respectively.

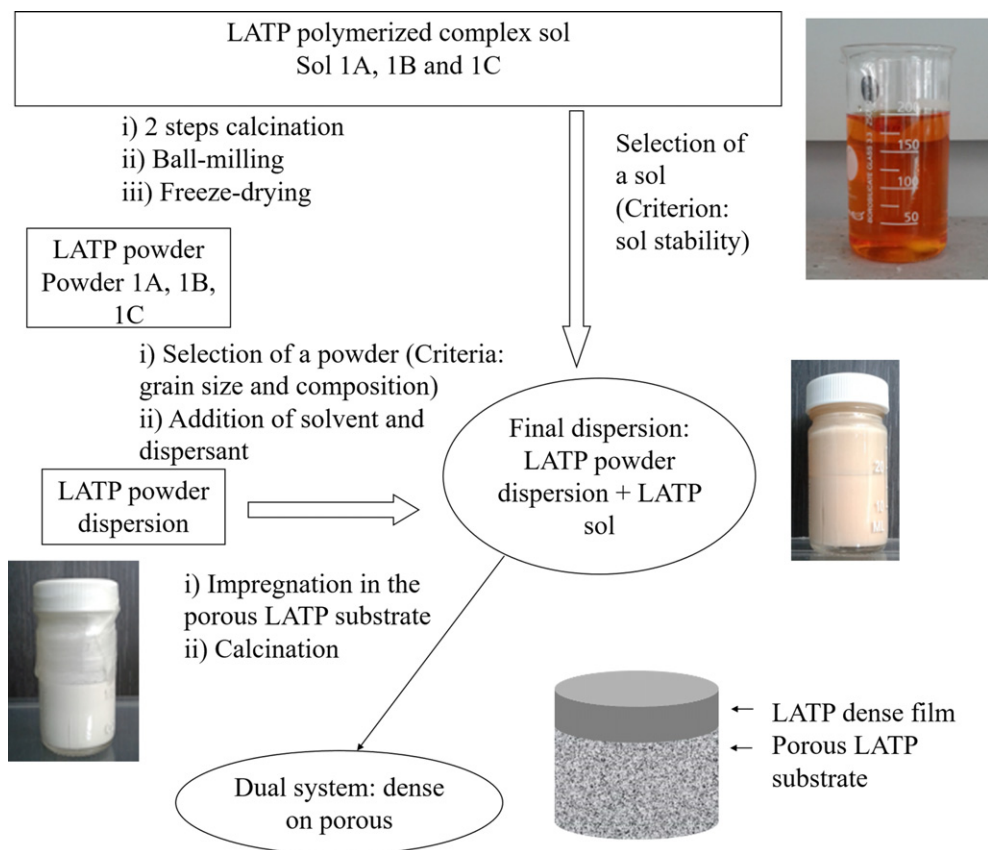


FIGURE 1 Preparation of LATP dual dense/porous system. [Color figure can be viewed at wileyonlinelibrary.com]

After thermal treatment at 80°C, transparent brown solutions were obtained for 1B and 1C and an opaque brown dispersion is obtained for 1A.

2.3.3 | Powders preparation (powder 1A, 1B, 1C)

The same polymerized complex method as described above was used for LATP powder preparation. The powders were prepared via calcination of the precursors sols 1A, 1B, and 1C. A 700°C calcination temperature was chosen from the literature.¹⁵ The use of a calcination temperature for the powder much lower than the sintering temperature of the membrane ($T_{\text{sintering}}=1100^{\circ}\text{C}$) is expected to limit grain growing thus enhancing their reactivity and favoring densification of the coating after thermal treatment. The sols were sintered in two steps: (i) a removal of the organic residues at 450°C during 7 hour and (ii) a calcination at 700°C during 2 hour (rising rate 100°C/h). Between these two steps, the powder was manually grinded in a mortar.

For simplification, the different powders obtained from calcination of sol 1A, 1B, and 1C are named powder 1A, powder 1B, and powder 1C, respectively.

2.3.4 | Powder dispersion and final dispersion preparation

The following steps consisted in grinding the LATP powder by ball milling for 1 hour (400 tr/min, 13 mm agate balls, in ethanol) and freeze drying it for 2 hour after liquid nitrogen cooling. Then, this powder was dispersed into a MEK-ethanol azeotrope with 2 m% polyvinylpyrrolidone PVP K12 dispersant. The proportions are 1/1 w/w powder/solvents. Mechanical stirring (900 rpm, 72 hour) was then performed to homogenize the solution. This results in a dispersion of powder in an alcoholic medium. The final dispersion was then prepared by addition of the LATP sol in the LATP powder dispersion. The selection of the sol (criterion: sol stability) and powder (criteria: powder grain size and composition) is described in the Results paragraph. The mass ratio R_m , defined by the ratio LATP sol/(LATP sol + dispersion), was equal to 0.1.

2.3.5 | Preparation of LATP membrane on porous LATP substrate

Deposition of the LATP dispersion on top of the LATP porous substrate was made by dip coating at a 30 cm/min withdrawal speed. After coating, the samples were dried at 50°C during 15 minute. The heat treatment was then optimized to promote the removal of organic compounds with a dwell at 600°C for 2 hour and the densification of the layers with a thermal treatment at 1 hour at 1100°C (temperature rising

rate 100°C/h). This layer was waterproof as tested by a drop test experiment: no water infiltration was detected.

2.4 | Ionic conductivity

In the lithium-air battery, the porous LATP substrate is impregnated with a liquid electrolyte so that it is not the limiting factor for the dual system conductivity. This is why the measurements performed in this study aim at determining the ionic conductivity of the dense LATP membrane only. The Van der Pauw configuration was chosen for this purpose as it is a method generally applied to measure the conductivity in in-plane configuration.²⁶

It is worth noting that the Van der Pauw theory has been further explored by Riess and Tannhauser to extend its application from electronic conductors to mixed ionic-electronic solid conductors.²⁷ Bruce et al.²⁸ and Poulsen et al.²⁹ showed in particular that this method with four probes in in-plane configuration is valid for the measurement of ionic conductivity of solid electrolytes as demonstrated for PEO-LiCF₃SO₃, vitreous Ag₇I₄AsO₄, and zirconia.

In the Van der Pauw configuration, four electrical contacts A, B, C, and D are located at arbitrary positions along the edge of a flat conductor of any shape.

The resistivity is calculated by the formula²⁶:

$$\rho = (\pi d / 2 \ln 2) (R_{AB,DC} + R_{BC,AD}) f(R - \text{ratio})$$

with ρ the resistivity of the sample in $\Omega\text{-cm}$, d its thickness in cm, $R_{AB, DC}$ in ohm is the potential difference between contact D and C divided by the current flowing through A and B, $f(R - \text{ratio})$ is the ratio of the two resistances $R_{AB, DC}$ and $R_{BC, AD}$.

In practice, some discrepancies with theory are expected as: (i) the contacts are not infinitively small and (ii) they are not located exactly at the edge of the sample. Anyway, Van der Pauw has considered these variations in its theory showing that a maximum of 10% error occurs for contacts size distance to the edge smaller than 1 mm.²⁶ These conditions were easily achieved.

Van der Pauw method is most often used applying a dc signal, which does not allow splitting the different contributions, such as the bulk resistance and the grain boundary resistance. To overcome this point, we used an ac signal (through an impedancemeter) to be able to obtain a whole range of impedance data. The $R_{AB, DC}$ and $R_{BC, AD}$ values for resistivity calculus were extracted from impedance fits.

3 | RESULTS

3.1 | Stability of the polymerized complex sols

As described above, for the LATP sols, the first criterion is to get a stable sol without precipitation. For this purpose, rheological measurements at room temperature were undertaken to

control the sol stability and rheological behavior with time. These measurements provide information on the mechanism at stake for the different behavior of sols 1A and 1B/1C.

As expected from first observations, L ATP sols have different rheological behaviors depending on the phosphate precursors used for their preparation (Figures 2 and 3). Sols made from trimethylphosphate (1B) and triethylphosphate (1C) exhibit a viscosity as low as 7 ± 1 mPa·s (at 320 seconds^{-1}) that remains stable for more than 600 hour (25 day). Sol 1A is more viscous (14 mPa·s at 320 seconds^{-1}) and not stable: an increase in viscosity of 100% within 25 day was measured. Moreover, the rheological study (Figure 2) brings out the thixotropic character of sol 1A, with a hysteresis area of 9%. This thixotropic behavior has been related to the presence of agglomerates in the mixture that are broken at higher shear rates.³⁰ The lower viscosity as well as the smaller hysteresis for sol 1B and 1C confirm that only few aggregates are present. Besides, this is in good agreement with SEM images showing the formation of large aggregates in the range 500-800 nm (Figure 4) for 1A powder.

Sols 1B and 1C have similar rheological behaviors: high stability, low viscosity, and low hysteresis. The absence of aggregates in sol 1B and 1C is attributed to the lower reactivity of trimethyl and triethyl phosphate ester toward hydrolysis as compared to phosphoric acid.³¹ Sol 1B and 1C are both interesting as L ATP precursor solution in the final dispersion; so that in the following, the sol with trimethylphosphate precursor (1B) was arbitrarily chosen for this purpose.

3.2 | Morphology of L ATP powders

For the L ATP powder selection, two criteria have been taken into account: the granulometry of the powders and their composition.

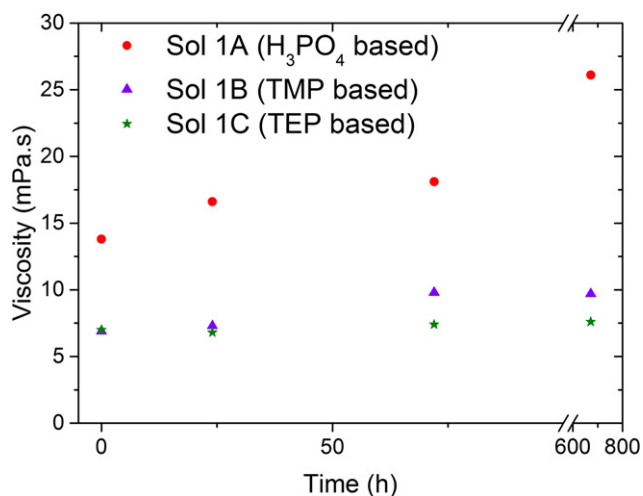


FIGURE 2 Viscosity as a function of time for the precursor solutions 1A (H₃PO₄), 1B (TMP), and 1C (TEP). Shear rate 322 seconds^{-1} [Color figure can be viewed at wileyonlinelibrary.com]

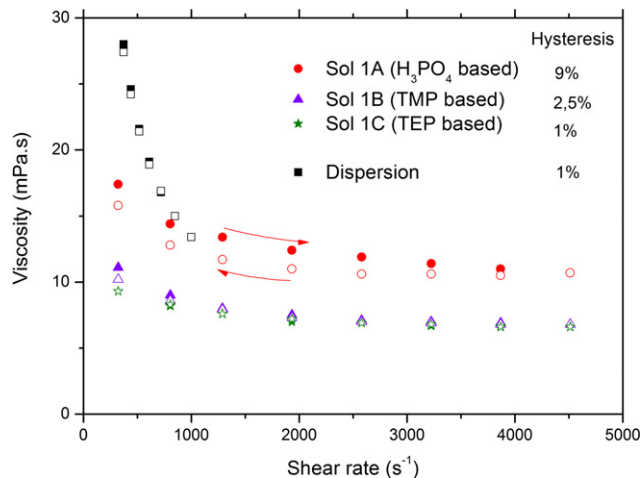


FIGURE 3 Viscosity as a function of applied shear rate for the sols 1 hour after their preparation, first by increasing shear rate then decreasing shear rate. Plain labels: increasing shear rates, void labels: decreasing shear rates. [Color figure can be viewed at wileyonlinelibrary.com]

SEM images of the powder 1A are presented in Figure 4A,B. Two populations of grains are observed with mean grain sizes of 50 and 500 nm. By comparison, the powders obtained from calcination of sol 1B and 1C present a much finer microstructure with grain size around tens of nanometers (Supplemental Information, Figure S1). The largest grains of powder 1A are the result of the observed precipitation of the sol. As stated before, grains sizes typically of hundreds of nanometers are expected to be favorable to both conductivity of the membrane and dispersion stability, only the powder 1A respects this criteria.

In addition to the required grain size, powder 1A benefits from a low level of impurities after annealing as evidenced by XRD (cf Figure 4C), showing only some Bragg peaks corresponding to Li₄P₂O₇.

Having the required grain size and composition, powder 1A is selected for the preparation of the dispersion in the following.

3.3 | Stability of L ATP powder dispersions

The final L ATP dispersion has been prepared following the protocol described in the paragraph II.III, with the selected sol 1B [(CH₃)₃PO₄ precursor] and powder 1A (H₃PO₄ precursor).

The stability of the final dispersion has been controlled by sedimentation speed experiments (with a measurement method based on the multiple light scattering, Turbiscan device) and rheological measurements. Sedimentation speed calculated from Turbiscan experiments (not shown here) is low (10^{-8} m/s). The hysteresis ratio calculated on the viscosity vs shear rate curve remains low (1%, see Figure 3). This very low thixotropic behavior is the signature of a stable dispersion with agglomerates size that remains

quasiunchanged whatever the shear force applied. This is also the evidence that this protocol with the selected sol 1B and powder 1A is suitable for the preparation of dispersion stable enough for the application.

3.4 | Microstructure of the LATP dual dense/porous system

The microstructure of the samples was observed by FEG-SEM. As an illustration, the images of a cross section of the porous support (Figure 5A) and of the dense membrane (Figure 5B) are given. In the porous part (Figure 5A), porosity

ratio of $30\% \pm 5\%$ and pore sizes in the range 1-10 μm are observed, this is similar to the porosity generally observed for porous LATP substrate provided by CTI after annealing at 1100°C . This demonstrates that the porosity of the substrate was not clogged by the LATP dense membrane preparation process. At the top of the sample, a dense layer is observed (Figure 5B). The densification of the layer was associated with an increase in the grain size from 50 to 500 nm (powder 1A) to a mean grain size in the film of 1.5 μm , with a rather large distribution (standard deviation 0.78 μm , $d_{99}=3.3 \mu\text{m}$). The maximum grain size is 5 μm . These values are expected to be favorable to

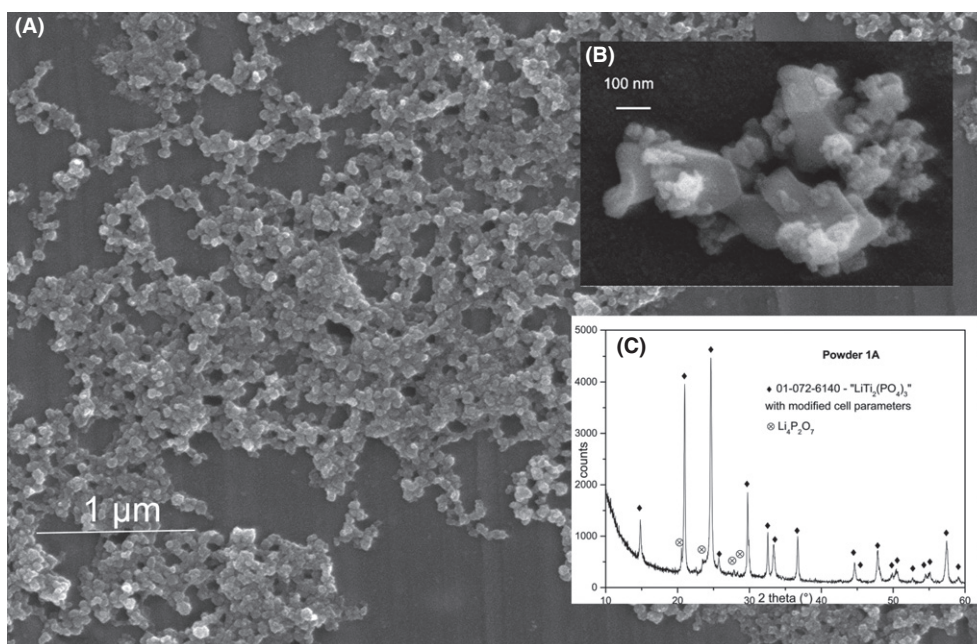


FIGURE 4 LATP powder 1A (H_3PO_4) phosphate precursor: (A), (B) FEG-SEM images, (C) XRD diagram.

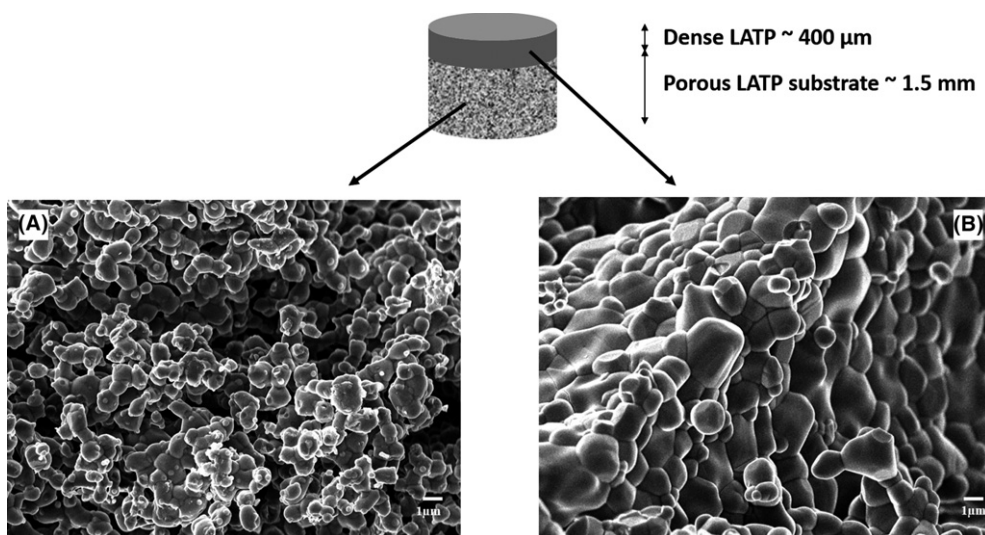


FIGURE 5 SEM images of (A) porous LATP CTI, after annealing at 1100°C , (B) deposited LATP layer after annealing at 1100°C .

high ionic conductivity as, from Jackman et al.,²⁵ an optimal grain size of less than or equal to 1.6 μm is expected to avoid microcracked grain boundaries in LATP.

By scanning the whole sample (cf Figure S2 in Supplemental Information), a thickness of $\sim 400 \mu\text{m} \pm 25 \mu\text{m}$ was determined for the dense layer. The porosity evolves from the bottom (CTI porous support, 30%-40% porosity, pore size 2-10 μm) to the top (LATP dense layer, no porosity visible at the scale of the measurement) with an intermediate layer around 50 μm thick. As required, the coating process leads to an infiltration limited to the top of the CTI support. The thickness of the dense layer could be tuned by changing the processing parameters.

3.5 | Analysis of phases

XRD pattern of the LATP membrane is presented in Figure 6 in addition to the XRD of the powder 1A. Crystalline LATP is detected and refined cell parameters [$a=8.48 \text{ \AA}(3)$;

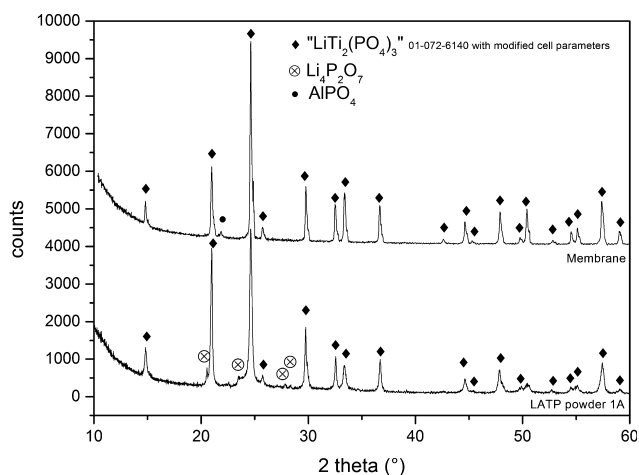


FIGURE 6 XRD pattern at room temperature of LATP powder (annealing 700°C) and LATP films (annealing 1100°C, 1 hour)

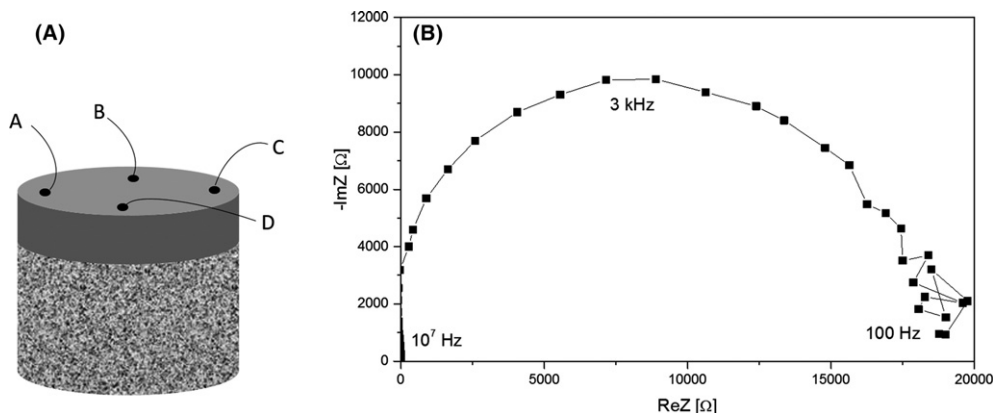


FIGURE 7 (A) Measurement configuration. (B) Nyquist plot of the impedance spectroscopy measurement on the LATP double-layer system $-\Delta V=60 \text{ mV}$.

$c=20.76 \text{ \AA}(3)$] are in agreement with reported ones for the composition $\text{Li}_{1+x}\text{Al}_x\text{Ti}_{2-x}(\text{PO}_4)_3$, $x=0.3$.³² AlPO_4 is detected after the heat treatment at 1100°C. However, Li-rich phase $\text{Li}_4\text{P}_2\text{O}_7$ that was detected in the 1A powder is not present in the film as $\text{Li}_4\text{P}_2\text{O}_7$ melts at 885°C.³³ As shown by several studies, the presence of some AlPO_4 is not detrimental to LATP conductivity or even slightly beneficial to syntheses reproducibility.³⁴⁻³⁶

3.6 | Ionic conductivity by van der Pauw method

3.6.1 | Validation of the AC-Van der Pauw configuration for LATP ionic conductivity measurement

Due to the lack of information regarding the use of ac-Van der Pauw configuration for conductivity measurement, we first performed measurements on SPS sintered pellet of LATP (protocol has been described elsewhere¹⁵) using two kinds of configurations for sake of comparison: face-to-face geometry and Van der Pauw geometry. For Van der Pauw geometry, four silver dots of 1 mm diameter were deposited at the edge of a 1.26-mm-thick pellet of diameter 15 mm. The pellet is 99% dense and was polished before ionic conductivity measurements.

The Nyquist plots obtained from impedance measurements in face-to-face configuration (a) and in Van der Pauw configuration (b) are given in Supplementary Information. In both cases a semicircle is obtained at frequencies between 100 and 10^7 Hz with, however, different shapes. While a well-defined semicircle in Van der Pauw configuration is observed; in face-to-face configuration, the semicircle is deformed which could arise from the presence of a second RC element. This demonstrates the higher anisotropy of the conductivity perpendicular to the plan as compared to the in-plane conductivity. This

result is in accordance with anisotropic grain growth observed in field-assisted sintering of LATP by Rosenberger,⁵ which is a technique similar to SPS in the sense of the application of a nonisotropic electrical field. A fit with an $R_0 + R_1//C_1$ equivalent electrical circuit, with R_0 the electrical resistance of the measurement circuit, R_1 the resistance of the electrolyte, and C_1 the corresponding capacitor, was performed. Taken into account the 1.26 mm thickness of the sample, a conductivity of 2.6×10^{-4} S/cm is obtained in Van der Pauw configuration as compared to 2.4×10^{-4} S/cm in face-to-face configuration. This 8% error between the two measurement methods is within the expected error (10%) for Van der Pauw experiments.

3.6.2 | Ionic conductivity of LATP membrane on LATP porous substrate

The Van der Pauw setup with impedance measurement being validated for LATP membranes, it was used for the characterization of the dual porous/dense system.

A semicircle is obtained in the Nyquist plot at frequencies between 100 and 10^7 Hz (Figure S3 of Supplemental Information). The fit with an $R_0 + R_1//C_1$ equivalent electrical circuit gives a value of $16\,500 \, \Omega \pm 500$ (mean value and standard deviation for eight measurements) for R_1 (electrolyte resistance). The LATP top layer being 400 μm thick, the conductivity of the LATP is calculated to be 3.3×10^{-4} S/cm. Taken into account the error on the thickness measurement ($\pm 50 \, \mu\text{m}$), a conductivity from 1×10^{-4} S/cm to 5×10^{-4} S/cm is calculated.

4 | CONCLUSION

To achieve both high mechanical properties and low ionic resistance, a dual system with a dense and highly conductive solid electrolyte top layer on a porous mechanical support was designed. The LATP top-layer conductivity attains 1 to 5×10^{-4} S/cm which is among the best conductivities reported for LATP, the best total conductivity in the literature being 7×10^{-4} S/cm for solid state³ and sol-gel methods.²⁵ It is noteworthy that in our work these high ionic conductivity performances have been obtained on a porous support, so that this process could be compatible with lower thickness of LATP top layer and then lower ionic resistance. The high ionic conductivity performances are attributed to the high purity level of LATP (only some AlPO_4 secondary phase detected), an optimal grain size, and high densification levels obtained via both a fine control of the wet chemistry process parameters (active LATP precursors-based matrix) and optimization of the calcination step.

The coupling of the impedance method with the Van der Pauw configuration has been demonstrated as an up-to-date tool for a more informative measurement of the conductivity of solid electrolytes in particular in such dual dense/porous systems.

The versatile double-layer system preparation method and impedance Van der Pauw measurements methods could advantageously be adapted to other types of solid electrolytes or application fields, such as batteries, fuel cells, and electrolyzers, for a precise control of the microstructure and ionic conductivity of dense/porous systems.

ACKNOWLEDGMENTS

We thank the company CTI for the preparation of the porous substrates, Lionel Presmanes (CIRIMAT) for Van der Pauw experiments, and the French Research Agency (ANR) for its financial support in the framework of the LiO_2 project.

REFERENCES

1. Bruce PG, Freunberger SA, Hardwick LJ, Tarascon J-M. Li-O₂ and Li-S batteries with high energy storage. *Nat Mater*. 2012;11:19–29.
2. Jackman SD, Cutler RA. Stability of NaSICON-type $\text{Li}_{1.3}\text{Al}_{0.3}\text{Ti}_{1.7}\text{P}_3\text{O}_{12}$ in aqueous solutions. *J Power Sources*. 2013;230:251–260.
3. Aono H, Sugimoto E, Sadaoka Y, Imanaka N, Adachi G. Ionic conductivity of solid electrolytes based on lithium titanium phosphate. *J Electrochem Soc*. 1990;137:1023–1027.
4. Soman S, Iwai Y, Kawamura J, Kulkarni A. Crystalline phase content and ionic conductivity correlation in LATP glass–ceramic. *J Solid State Electrochem*. 2011;16:1761–1766.
5. Rosenberger A, Gao Y, Stanciu L. Field-assisted sintering of $\text{Li}_{1.3}\text{Al}_{0.3}\text{Ti}_{1.7}(\text{PO}_4)_3$ solid-state electrolyte. *Solid State Ion*. 2015;278:217–221.
6. Kosova NV, Devyatkina ET, Stepanov AP, Buzlukov AL. Lithium conductivity and lithium diffusion in NASICON-type $\text{Li}_{1+x}\text{Ti}_{2-x}\text{Al}_x(\text{PO}_4)_3$ ($x=0; 0.3$) prepared by mechanical activation. *Ionics*. 2008;14:303–311.
7. Schroeder M, Glatthaar S, Binder JR. Influence of spray granulation on the properties of wet chemically synthesized $\text{Li}_{1.3}\text{Ti}_{1.7}\text{Al}_{0.3}(\text{PO}_4)_3$ (LATP) powders. *Solid State Ion*. 2011;201:49–53.
8. Kunshina GB, Gromov OG, Lokshin EP, Kalinnikov VT. Sol-gel synthesis of $\text{Li}_{1.3}\text{Al}_{0.3}\text{Ti}_{1.7}(\text{PO}_4)_3$ solid electrolyte. *Russ J Inorg Chem*. 2014; 59:424–430.
9. Bucharsky EC, Schell KG, Hintennach A, Hoffmann MJ. Preparation and characterization of sol-gel derived high lithium ion conductive NZP-type ceramics $\text{Li}_{1+x}\text{Al}_x\text{Ti}_{2-x}(\text{PO}_4)_3$. *Solid State Ion*. 2015;274:77–82.
10. Kotobuki M, Isshiki Y, Munakata H, Kanamura K. All-solid-state lithium battery with a three-dimensionally ordered $\text{Li}_{1.5}\text{Al}_{0.5}\text{Ti}_{1.5}(\text{PO}_4)_3$ electrode. *Electrochim Acta*. 2010;55:6892–6896.
11. Huang L, Wen Z, Wu M, Wu X, Liu Y, Wang X. Electrochemical properties of $\text{Li}_{1.4}\text{Al}_{0.4}\text{Ti}_{1.6}(\text{PO}_4)_3$ synthesized by a co-precipitation method. *J Power Sources*. 2011;196:6943–6946.
12. Kotobuki M, Koishi M, Kato Y. Preparation of $\text{Li}_{1.5}\text{Al}_{0.5}\text{Ti}_{1.5}(\text{PO}_4)_3$ solid electrolyte via a co-precipitation method. *Ionics*. 2013;19:1945–1948.
13. Kotobuki M, Kobayashi B, Koishi M, Mizushima T, Kakuta N. Preparation of $\text{Li}_{1.5}\text{Al}_{0.5}\text{Ti}_{1.5}(\text{PO}_4)_3$ solid electrolyte via coprecipitation using various PO_4 sources. *Mater Technol*. 2014;29:A93–A97.
14. Kim KM, Shin DO, Lee Y-G. Effects of preparation conditions on the ionic conductivity of hydrothermally synthesized $\text{Li}_{1+x}\text{Al}_x\text{Ti}_{2-x}(\text{PO}_4)_3$ solid electrolytes. *Electrochim Acta*. 2015;176:1364–1373.

15. Duluard S, Paillassa A, Puech L, et al. , et al. Lithium conducting solid electrolyte $\text{Li}_{1.3}\text{Al}_{0.3}\text{Ti}_{1.7}(\text{PO}_4)_3$ obtained via solution chemistry. *J Eur Ceram Soc.* 2013;33:1145–1153.
16. Ohara NK, Lithium ion conductive glass ceramics: Properties and application in lithium metal batteries, presented at the Symposium on Energy Storage: Beyond Lithium Ion; Materials Perspective, Oak Ridge National Laboratory, October 7–8, 2010, <http://oharacorp.com/pdf/ohara-presentation-ornl-symposium-10-08-2010.pdf>. Accessed August 29, 2016.
17. Singhal SC. “Past Present and Future;” Chapter 1. In: Irvine JTS, Connor P, eds. *Solid Oxide Fuels Cells: Facts and Figures*. London: Springer Verlag; 2013:1–23.
18. Lenormand P, Caravaca D, Laberty-Robert C, Ansart F. Thick films of YSZ electrolytes by dip-coating process. *J Eur Ceram Soc.* 2005;25:2643–2646.
19. Cretin M, Fabry P. Comparative study of lithium ion conductors in the system $\text{Li}_{1+x}\text{Al}_x\text{A}_{2-x}\text{IV}(\text{PO}_4)_3$ with AIV=Ti or Ge and $0 \leq x \leq 0.7$ for use as Li^+ sensitive membranes. *J Eur Ceram Soc.* 1999;19:2931–2940.
20. Wu XM, Li XH, Wang SW, et al. Preparation and characterization of lithium-ion-conductive $\text{Li}_{1.3}\text{Al}_{0.3}\text{Ti}_{1.7}(\text{PO}_4)_3$ thin films by the solution deposition. *Thin Solid Films.* 2003;425:103–107.
21. Yokota O, Yashima M, Kakihana M, Shimofuku A, Yoshimura M. Synthesis of metastable tetragonal (t') ZrO_2 -12 mol% $\text{YO}_{1.5}$ by the organic polymerized complex method. *J Am Ceram Soc.* 1999;82:1333–1335.
22. Baqué L, Caneiro A, Moreno MS, Serquis A. High performance nanostructured IT-SOFC cathodes prepared by novel chemical method. *Electrochem Commun.* 2008;10:1905–1908.
23. Rieu M, Sayers R, Laguna-Bercero MA, Skinner SJ, Lenormand P, Ansart F. Investigation of graded $\text{La}_2\text{NiO}_{4+\delta}$ cathodes to improve SOFC electrochemical performance. *J Electrochem Soc.* 2010;157:B477–B480.
24. Zhai H-F, Tang R-L, Li A-D, Guo H-R, Xia Y-D, Wu D. Preparation and characterization of relaxor ferroelectric $0.65\text{Pb}(\text{Mg}_{1/3}\text{Nb}_{2/3})\text{O}_3$ - 0.35PbTiO_3 by a Polymerizable complex method. *J Am Ceram Soc.* 2009;92:1256–1261.
25. Jackman SD, Cutler RA. Effect of microcracking on ionic conductivity in LATP. *J Power Sources.* 2012;218:65–72.
26. Van der Pauw LJ. A method of measuring the resistivity and Hall coefficient on lamellae of arbitrary shape. *Philips Research Review.* 1958; 20:220–224.
27. Riess I, Tannhauser DS. Application of the van der Pauw method to conductivity measurements on mixed ionic-electronic solid conductors. *Solid State Ion.* 1982;7:307–315.
28. Bruce PG, Evans J, Vincent CA. A dc technique for measurement of solid electrolyte conductivity. *Solid State Ion.* 1987;25:255–262.
29. Poulsen FW, Buitink P, Malmgren-Hansen B. Van der Pauw and conventional 2-point conductivity measurements on YSZ-plates. In: Grosz F, Zegers P, Singhal SC, Yamamoto O, eds. *Proceedings of the 2nd International Symposium on Solid Oxide Fuel Cells*. Pennington, NJ: The Electrochemical Society; 1991: 755–767.
30. Gilleo KB. Fundamentals and testing, Chapter 1. In: Tracton AA, ed. *Coatings Technology Handbook*. 3rd edn. Boca Raton, FL: CRC Press; 2005: 1.1–1.12.
31. Knipe AC, Watts WE, *Organic Reaction Mechanisms 1998 - A. C. Knipe*. Hoboken, NJ: Wiley; 2003.
32. Arbi K, Mandal S, Rojo JM, Sanz J. Dependence of ionic conductivity on composition of fast ionic conductors $\text{Li}_{1+x}\text{Ti}_{2-x}\text{Al}_x(\text{PO}_4)_3$, $0 \leq x \leq 0.7$. A parallel NMR and electric impedance study. *Chem Mater.* 2002;14:1091–1097.
33. Tien TY, Hummel FA. Studies in lithium oxide systems: X, Lithium phosphate compounds. *J Am Ceram Soc.* 1961;44:206–208.
34. Fu J. Superionic conductivity of glass-ceramics in the system $\text{Li}_2\text{O}-\text{Al}_2\text{O}_3-\text{TiO}_2-\text{P}_2\text{O}_5$. *Solid State Ion.* 1997;96:195–200.
35. Thokchom JS, Kumar B. Water durable lithium ion conducting composite membranes from the $\text{Li}_2\text{O}-\text{Al}_2\text{O}_3-\text{TiO}_2-\text{P}_2\text{O}_5$ glass-ceramic. *J Electrochem Soc.* 2007;154:A331–A336.
36. Puech L, Cantau C, Vinatier P, Toussaint G, Stevens P. Elaboration and characterization of a free standing LiSICON membrane for aqueous lithium-air battery. *J Power Sources.* 2012;214:330–336.